Radiative stabilization following double-electron capture in slow Ne^{10+}+He collisions

J.-Y. Chesnel,[1] H. Merabet,[2,*] B. Sulik,[3] F. Frémont,[2] C. Bedouet,[2] X. Husson,[2] M. Grether,[1] and N. Stolterfoht[1]
[1]*Hahn-Meitner Institut GmbH, Bereich Festkörperphysik, Glienickerstrasse 100, D-14109 Berlin, Germany*
[2]*Laboratoire de Spectroscopie Atomique, 6 Boulevard du Maréchal Juin, F-14050 Caen Cedex, France*
[3]*Institute of Nuclear Research of the Hungarian Academy of Sciences, P.O. Box 51, H-4001 Debrecen, Hungary*
(Received 30 April 1998)

Individual contributions to radiative stabilization in $Ne^{10+}+He$ collisions were studied at projectile energies from 1 to 150 keV. In these collisions doubly excited states $3lnl'$ and $4lnl'$ ($n\geqslant 4$) can be produced by uncorrelated two-electron transitions or by dielectronic processes caused by the electron-electron interaction. Compared to our previous study of stabilization, we extended the projectile-energy range down to 1 keV and the present analysis is based entirely on experimental data. Radiative stabilization was evaluated by combining our recent results for Auger decay cross sections with available radiative and nonradiative branching ratios. The total amount of radiative stabilization was found to be nearly constant (≈ 0.35) within the studied energy range. However, the individual contributions to stabilization were found to change significantly. At 1 keV the major contribution to stabilization is shown to be due to the decay of the nonequivalent electron configurations $3lnl'$ ($n\geqslant 6$) produced during the collision by the dielectronic process of autoexcitation.
[S1050-2947(98)08010-X]

PACS number(s): 32.80.Hd, 34.50.Fa

I. INTRODUCTION

Charge exchange is at the heart of many important processes in atomic collisions, notably, electron capture by slow, multiply charged ions colliding with neutral atoms [1–10]. In the case of double electron capture, doubly excited states due to configurations $nln'l'$ of the projectile are created. After the collision, the doubly excited states decay either by photon emission or by Auger-electron emission. Radiative and nonradiative decay processes allow the investigation of the double-capture processes by means of photon spectroscopy [3–5,10] and Auger-electron spectroscopy [1,6,9]. Photon emission gives rise to the radiative stabilization of the electrons at the projectile ions. The study of the pathways leading to radiative stabilization is essential for understanding various phenomena involved in x-ray and light emission from stars. Therefore, in the recent past, radiative stabilization of doubly excited states in few-electron systems has received an increasing attention and has been the subject of intensive discussions [6,7,11–17].

For the analysis of radiative stabilization following double-electron capture, it is useful to distinguish two categories of doubly excited configurations $nln'l'$, namely, those involving near-equivalent n values ($n'\approx n$) and those involving nonequivalent n values ($n'\gg n$). In the case of 1- to 150-keV $Ne^{10+}+He$ collisions, cross sections for producing configurations $nln'l'$ with $|n'-n|\leqslant 2$ are rather independent of the collision energy [18]. On the other hand, cross sections attributed to configurations with $|n'-n|>2$ increase strongly with decreasing impact energy [18]. Hence, for $Ne^{8+}(nln'l')$ ions we consider the case $|n'-n|>2$ separately from $|n'-n|\leqslant 2$ and denote the configurations corresponding to the latter case as near-equivalent electron configurations. Note that the expression ''near-equivalent'' includes the case $n=n'$.

For these near-equivalent electron configurations, the Auger yield $a_{nln'l'^1L}$ for the state $nln'l'^1L$ is close to unity [6] and, hence, the related fluorescence yield is rather weak. This has experimentally been verified by Fléchard *et al.* [17] and Abdallah *et al.* [19] for the configurations $3l4l'$, $3l5l'$, and $4l5l'$ of Ne^{8+} ions. The situation is quite different for nonequivalent electron configurations that include a core electron and a high-lying Rydberg electron. In this case, due to the small overlap of the corresponding wavefunctions, the interaction between the electrons is reduced. Therefore, the probability for photon emission becomes important, and the fluorescence yields associated with nonequivalent electron configurations are likely to be significant [6]. For instance, fluorescence yields $\omega_{3lnl'}$ as large as 0.5 have been obtained for the radiative transitions from initial states formed by the configurations $3lnl'$ ($n\geqslant 6$) of the ion Ne^{8+} [17,19,20]. Thus, radiative stabilization can play an important role for double-capture processes into multicharged ions when the production of nonequivalent electron configurations is relatively large [6,16].

For the production of doubly excited states $nln'l'$ of the projectile ion, two kinds of double-capture mechanisms, referred to as monoelectronic and dielectronic processes, are considered. In Fig. 1, these mechanisms are depicted schematically for the example of $Ne^{10+}+He$ collisions. In the incident channel two electrons occupy the $1s$ orbital of the target He. During the collision, two independent monoelectronic transfers due to nucleus-electron interactions give rise to near-equivalent electron configurations $3lnl'$ and $4lnl'$ with $n=4$ and 5 at intermediate internuclear distances of typically 4 to 10 a.u. [9,18]. On the other hand, dielectronic processes lead to simultaneous *two-electron* transitions (Fig. 1) where the mutual interaction between the electrons plays an essential role [9,18]. Although dielectronic processes can produce near-equivalent electron configurations [18], dielec-

*Present address: Department of Physics/220, University of Nevada, Reno, NV 89557-0058.

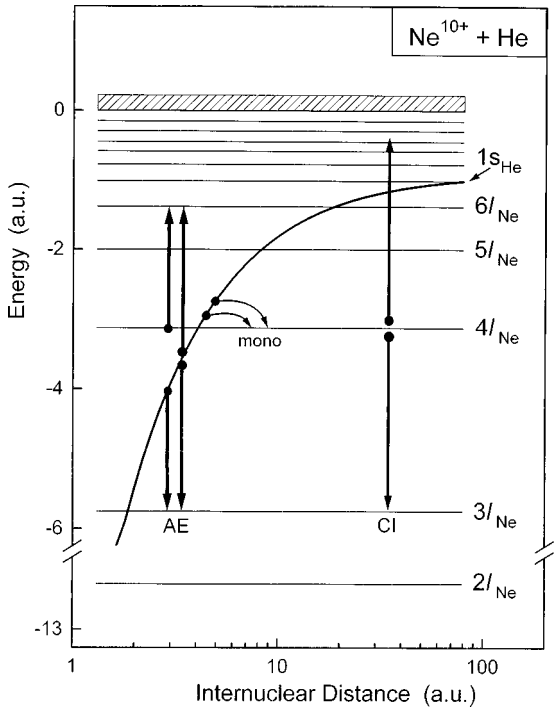

FIG. 1. Diagram of approximate orbital energies for the system $Ne^{10+}+He$. The inclined arrows illustrate two independent monoelectronic transfers due to nucleus-electron interactions. The monoelectronic processes (mono) produce configurations $nln'l'$ of equivalent and near-equivalent electrons. Simultaneous two-electron transitions due to the electron-electron interaction are depicted by using vertical arrows. The collisional AE process gives rise to the series $3lnl'$. In the postcollisional and asymptotic regions, CI phenomena occur between the configurations $4l4l'$ and high-lying Rydberg states $3lnl'$ $(n\geqslant 10)$.

tronic processes lead primarily to nonequivalent electron configurations $3lnl'$ involving high-lying Rydberg states (Fig. 1). A characteristic example of dielectronic processes is autoexcitation (AE) [6], where one electron is transferred to a deeper-lying level, while the second electron is excited to a higher-lying Rydberg level.

In the case of the dielectronic mechanisms, significant differences occur with respect to the n ranges of the populated Rydberg states and with respect to the internuclear distances at which the transitions take place. First, during the collision the dielectronic process of AE creates the Rydberg states $3lnl'$ with significant probabilities for n values in the range from 6 to 9 [9,18]. Higher Rydberg states $(n\geqslant 10)$ are also produced by AE with smaller probabilities. Second, in the postcollisional region a dielectronic process caused by configuration interaction (CI), also referred to as autotransfer to Rydberg states (ATR) [21,22], produces two-electron transitions from the initially populated configurations $4l4l'$ to the Rydberg series $3lnl'$ with n values ranging from 10 to about 12 [23]. This postcollisional CI process occurs in the range of internuclear distances from typically 10 to 20 a.u. Finally, in the asymptotic region of large internuclear distances $(\gtrsim 20$ a.u.), CI occurs in the free projectile ion between $4l4l'$ and Rydberg states $3lnl'$ involving levels with $n\gtrsim 12$ [12,24].

Since the corresponding fluorescence yields are significant, the production of nonequivalent electron configurations $3lnl'$ plays an important role for radiative stabilization. In the early studies of radiative stabilization for 10-keV $Ne^{10+}+He$ collisions, the postcollisional CI process (also called ATR) was considered as an important mechanism that enhances the radiative-decay branch of the components $4l4l'$ by producing $3lnl'$ states with large fluorescence yields [10,21]. Since for the impact energy of 10 keV the configurations $4l4l'$ were assumed to be predominantly populated during the collision, it was concluded that this postcollisional process induces the largest contribution to radiative stabilization [21]. However, this claim has been shown to be questionable [12,16,18,25]. Van der Hart *et al.* [25] have shown that the postcollisional CI mechanism actually populates $3lnl'$ components whose fluorescence yields are lower than those for components created by the asymptotic CI process and, thus, leads to a *weaker* radiative stabilization of $4l4l'$ than that expected in the asymptotic region. Furthermore, our recent Auger-electron-spectroscopy measurements [16,18] have shown that the production of configurations $3lnl'$ $(n=4-9)$ actually exceeds that of configurations $4l4l'$. Hence, besides postcollisional CI, additional processes have to be incorporated to explain the amount of radiative stabilization in $Ne^{10+}+He$ collisions.

In our previous work [16], the objective was to perform a comprehensive study of the different contributions to radiative stabilization which, before, had been treated rather separately by different groups [7,10–13,21]. Since only theoretical values [20] were available for Auger and fluorescence yields, we consider our study [16] as an initial step for a comprehensive analysis of the radiative stabilization in $Ne^{10+}+He$ collisions. The main goal of the present paper is to complement this previous study [16] by providing contributions to stabilization based exclusively on experimental data. In particular, experimental Auger and fluorescence yields measured recently by Abdallah *et al.* [19] by means of the recoil-ion-momentum spectroscopy are presently used. Furthermore, the analysis of stabilization is extended to impact energies one order of magnitude smaller than those previously investigated [16]. The results obtained at these very low energies are shown to confirm the conclusions made in Ref. [16] at the higher projectile energy of 10 keV.

As already emphasized in Ref. [16], it is noted that we use the term ''fluorescence yield'' to denote the radiative branching ratio for individual states, while the notation ''radiative-stabilization value'' refers to the mean branching ratio for radiative decay with respect to the *total* number of populated doubly excited states.

II. SPECTRA AND DATA ANALYSIS

A. High-resolution spectra

Figure 2 shows high-resolution L-Auger spectra obtained recently for 1- and 10-keV $Ne^{10+}+He$ collisions [18]. These spectra were recorded at an angle of 40° with respect to the incident beam direction. It is noted that no significant anisotropy for the Auger line groups has been observed in the angular region from 30° to 90° [18]. The line intensities originate from the Auger decay of the nonequivalent electron configurations $3lnl'$ $(n\geqslant 6)$ and the components $4l4l'$, which decay to the $2l\varepsilon l'$ continuum by means of L-Auger transitions. It is seen that the peaks associated with the con-

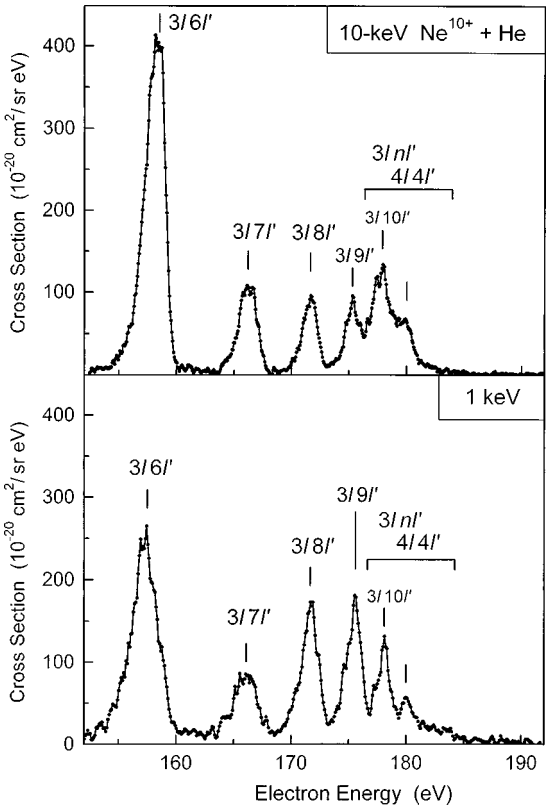

FIG. 2. High-resolution spectra of L-shell Auger electrons produced in $Ne^{10+}+He$ collisions at projectile energies of 1 and 10 keV. The detection angle is 40° with respect to the incident beam direction. The peaks are associated with the configurations $3lnl'$ ($n\geqslant 6$). The peak group at 178–180 eV corresponds to the configurations $4l4l'$ and the series limit of the configurations $3lnl'$ ($n\geqslant 10$). For the electron energy range from 145 to 200 eV the line intensities are not affected by double-collision effects (see Ref. [18]).

figurations $3lnl'$ ($n=6$ to 9) are well separated from the group of peaks due to the overlapping components $3lnl'$ ($n\geqslant 10$) and $4l4l'$ and centered at $\sim$178–180 eV (Fig. 2). While Auger emission associated with the configurations $3l6l'$ and $3l7l'$ is reduced at 1 keV in comparison with 10 keV, Auger intensities due to the configurations $3l8l'$ and $3l9l'$ are found to increase when the impact energy decreases (Fig. 2). More specifically, it is seen that at 1 and 10 keV the Auger contribution due to nonequivalent electron configurations $3lnl'$ ($n=6-9$) is significantly larger than that due to the overlapping components $3lnl'$ ($n\geqslant 10$) and $4l4l'$.

In addition to the lines intensities due to the configurations $3lnl'$ ($n\geqslant 6$) and $4l4l'$, Auger emission from the configurations $3l4l'$, $3l5l'$, and $4lnl'$ ($n\geqslant 5$) was observed at electron energies from 15 to 145 eV. Spectra including these additional Auger line intensities have been presented in Ref. [18]. For a projectile energy of 150 keV, these spectra show that Auger emission from $3l4l'$, $3l5l'$, and $4lnl'$ ($n\geqslant 5$) is larger than that from the states $3lnl'$ ($n\geqslant 6$). In contrast, at the lower impact energy of 10 keV, Auger emission attributed to the states $3lnl'$ ($n\geqslant 6$) has been shown to become dominant [18]. This finding indicates that the production of nonequivalent electron configurations $3lnl'$ ($n=6-9$) by means of the collisional dielectronic AE process is significant at few-keV projectile energies. Hence, the photon emission from these configurations may give rise to an important contribution to radiative stabilization.

It is remarked here that the internal structure of the line groups attributed to $4l5l'$, $3l4l'$, and $3l5l'$ has been observed to change with respect to the impact energy [18], indicating that the l and l' populations depend on the collision energy. Therefore, the *average* branching ratios for radiative and nonradiative decays of the different configurations n,n' (summed over l and l') may vary with respect to the collision energy. In the following, this possible energy dependence of the *average* fluorescence and Auger yields is considered.

B. Cross-section determination

1. Auger-emission cross sections and Auger yields

The measured doubly differential electron spectra were used to evaluate the corresponding cross sections as described in Refs. [18,26,27]. First, the Auger spectra were integrated over electron energy to determine single-differential cross sections $d\sigma^a_{n,n'}/d\Omega$ for Auger-electron emission attributed to a given configuration n,n' (summed over l and l'). Then, total cross sections for Auger-electron emission $\sigma^a_{n,n'}$ were evaluated by integration of $d\sigma^a_{n,n'}/d\Omega$ over the electron-emission angle [18]. These cross sections $\sigma^a_{n,n'}$ are given in Table I. The absolute uncertainties for the evaluated total cross sections are about $\pm 30\%$ and the relative uncertainties with respect to variation of the emission angle are typically $\pm 20\%$. Double collision effects and systematic errors caused by beam spread after the deceleration of the ions have been carefully analyzed and corrected for [18].

In Table I, our calculated Auger yields [20] are also compared with values extracted from the recent measurements performed by Abdallah and co-workers [19,28] by means of the method of recoil-ion-momentum spectroscopy (RIMS). The calculated values [20] and the experimental data [19,28] generally agree well. For the nonequivalent electron configurations $3lnl'$ ($n=6-8$), the differences between theory and experiment are smaller than 5%. For the near-equivalent electron configurations, the agreement is also good since the differences do not exceed 15%. A larger deviation occurs for the overlapping states $4l4l'$ and $3lnl'$ ($n\geqslant 10$), where a difference of 45% appears. Hence, in the following, particular attention is devoted to the analysis of the group of peaks including these overlapping states.

It should be noted that, in contrast to the case of the nonequivalent electron states, the average Auger yields associated with the near-equivalent electron states are close to unity. Hence, in this latter case, although the discrepancies between the calculated and experimental Auger yields $a_{n,n'}$ are small, the differences between the corresponding fluorescence yields ($\omega_{n,n'}=1-a_{n,n'}$) can be significant. The large uncertainties for $\omega_{n,n'}$ in the specific case of the near-equivalent electron states have been taken into account for the present evaluation of the corresponding contribution to radiative stabilization.

TABLE I. Auger-emission cross sections $\sigma^a_{n,n'}$ and double capture cross sections $\sigma_{n,n'}$ for the configurations $3lnl'$ and $4lnl'$ ($n \geqslant 4$) produced in 1-, 10-, and 150-keV $Ne^{10+}+He$ collisions [18]. The relative uncertainties are $\pm 20\%$. For the cross sections associated with the configurations $3l4l'$, $3l5l'$, and $4lnl'$ ($n \geqslant 5$), the uncertainties are about $\pm 35\%$ since the part of the spectra including these configurations (i.e., the electron energy range from 15 to 150 eV) is affected by double-collision intensities (see Ref. [18]). The average Auger yields $a_{n,n'}$, which were previously calculated [20], are presented on the right-hand side. Experimental Auger yields obtained at 150 keV by means of recoil-ion-momentum spectroscopy [19,28] are given in the last column. The experimental uncertainties for the Auger yields [19,28] are $\pm 10\%$.

Configurations	$\sigma^a_{n,n'}$ (10^{-17} cm^2)			$\sigma_{n,n'}$ (10^{-17} cm^2)				
$nln'l'$	1 keV	10 keV	150 keV	1 keV	10 keV	150 keV	$a_{n,n'}$ (calc.)	$a_{n,n'}$ (expt.)
$3l4l'+3l5l'$	10	7	8	12	8	10	0.7	0.8
$3l6l'$	10.5	11.3	2.3	16.9	18.2	3.7	0.60	0.62
$3l7l'$	3.7	3.1	1.5	6.7	5.6	2.7	0.56	0.55
$3l8l'$	4.5	2.3	0.8	9.0	4.6	1.6	0.52	0.5
$3l9l'$	3.9	1.8	0.5	8.3	3.8	1.1	0.47	
$3lnl'$ $(n \geqslant 10)+4l4l'$	4.8	5.3	4.4	11.4	12.6	10.5	0.71	0.42
$4l5l'$	6.7	4.5	5.0	7.3	4.9	5.4	0.91	0.92
$4lnl'$ $(n \geqslant 6)$	4.5	4.9	3.9	5.0	5.4	4.3	0.8	0.9

As already mentioned in Sec. II A, the *average* Auger and fluorescence yields may vary with respect to the collision energy, as the l and l' populations depend on the energy. Therefore, in our previous calculations [20,29], the energy dependence of the average Auger yields $a_{n,n'}$ was investigated by evaluating the evolution of the occupation probabilities $q_n(l)$ and $q_{n'}(l')$ associated with the angular momenta l and l' of the configurations $nln'l'$. Because of the high number of substates belonging to the complexes n,n' presently studied, the variation of the average Auger yields $a_{n,n'}$ with respect to the energy dependence of the occupation distributions $q_n(l)$ and $q_{n'}(l')$ was found to be practically smoothed out in the averaging procedure [20,29]. Hence, we concluded that the average Auger yields are insensitive to the precise distributions $q_n(l)$ and $q_{n'}(l')$ and, in turn, rather independent of the projectile energy [16,20,29]. This conclusion has partially been confirmed in recent RIMS experiments by Hennecart *et al.* [30] who found practically the same average Auger yields at the projectile energies of 50 and 150 keV.

Consequently, the average fluorescence yields are expected to be rather independent of the projectile energy. This expectation is particularly valid for the nonequivalent electron complexes $(3,n)$ with $n=6$ to 9 for which a small variation of the average Auger yields is uncritical for the fluorescence yields, as the Auger yields are close to 0.5. However, the situation is different for the near-equivalent configurations for which the average Auger yields are larger than 0.8. In this specific case, a slight energy dependence of the average Auger yields may give rise to a significant energy dependence of the related fluorescence yields. In the following, after evaluation of the contribution to radiative stabilization originating from the decay of the near-equivalent electron configurations, the effects of a possible energy dependence for the average fluorescence yields is discussed.

2. Double-capture cross sections

Double-electron-capture cross sections $\sigma_{n,n'}$ were determined by dividing the Auger-emission cross sections $\sigma^a_{n,n'}$ by the corresponding average Auger yield $a_{n,n'}$ [18]. Since the average Auger yields were previously found to be practically independent of the collision energy, average Auger yields obtained experimentally at an energy of 150 keV [19,28] have been used to evaluate the cross sections $\sigma_{n,n'}$ also for collision energies lower than 150 keV [18]. The results for $\sigma_{n,n'}$ are given in Table I.

Particular care was taken to account for configuration interaction between $4l4l'$ and $3lnl'$ ($n \geqslant 10$). The group of peaks centered at $\sim$178–180 eV (Fig. 2) was integrated over electron energy and observation angle to determine the total cross section σ^a_{os} for Auger-electron emission from the *overlapping states* $4l4l'$ and $3lnl'$ with $n \geqslant 10$. In addition, the recent RIMS measurements [19,28] provided experimental values for the average Auger and fluorescence yields [a_{os} and ω_{os}] attributed to the overlapping states $4l4l'$ and $3lnl'$ ($n \geqslant 10$) (see Table I). Hence, the cross section σ^x_{os} for radiative emission from $4l4l'$ and $3lnl'$ ($n \geqslant 10$) can be evaluated from the results obtained for σ^a_{os}:

$$\sigma^x_{os} = \sigma^a_{os}\omega_{os}/(1-\omega_{os}). \tag{1}$$

Now, the emission cross sections σ^a_{os} and σ^x_{os} can be described as summations over three different contributions:

$$\sigma^a_{os} = \sigma_{3,n\geqslant 10}\, a_{3,n\geqslant 10} + \sigma_{4,4}\tau a_{3,n\geqslant 10} + \sigma_{4,4}(1-\tau)a_{4,4}, \tag{2a}$$

$$\sigma^x_{os} = \sigma_{3,n\geqslant 10}\omega_{3,n\geqslant 10} + \sigma_{4,4}\tau\omega_{3,n\geqslant 10} + \sigma_{4,4}(1-\tau)\omega_{4,4}. \tag{2b}$$

In these summations, the first terms $\sigma_{3,n\geqslant 10}a_{3,n\geqslant 10}$ and $\sigma_{3,n\geqslant 10}\omega_{3,n\geqslant 10}$ account, respectively, for the Auger- and radiative-emission cross sections associated with the configurations $3lnl'$ ($n \geqslant 10$) created by the collisional autoexcitation process. The quantity $\sigma_{3,n\geqslant 10}$ is the corresponding cross section (summed over n) for populating the states $3lnl'$ ($n \geqslant 10$) by means of AE. The Auger and fluorescence yields $a_{3,n\geqslant 10}$ and $\omega_{3,n\geqslant 10}$, respectively, are average yields over the angular momenta l and l' as well as over the principal quantum number n for values $n \geqslant 10$.

The second terms $\sigma_{4,4}\tau a_{3,n\geqslant 10}$ and $\sigma_{4,4}\tau\omega_{3,n\geqslant 10}$ in Eqs. (2) refer, respectively, to the Auger- and photon-emission cross sections for the Rydberg components $3lnl'$ $(n\geqslant 10)$ created by postcollisional and asymptotic CI mechanisms. The quantity $\sigma_{4,4}$ is the total cross section for producing the doubly excited states $4l4l'$ in the collisional region. The constant τ refers to the total fraction of the initial $4l4l'$ population that goes into the nonequivalent electron configurations $3lnl'$ $(n\geqslant 10)$ by CI. In a recent study [23], this fraction was found to be equal to ~ 0.6. Since CI is likely to create Rydberg components $3lnl'$ with higher n values than the collisional AE process, the corresponding average yields $a_{3,n\geqslant 10}$ and $\omega_{3,n\geqslant 10}$ may depend on the production mechanisms. However, for the present analysis, it is useful to determine the lower limit for the contribution to radiative stabilization due to the decay of configurations produced by the AE process. Thus, AE is assumed to produce only states $3lnl'$ with $n<10$. In other words, the cross section $\sigma_{3,n\geqslant 10}$ is supposed to be negligible and, hence, the AE terms of Eqs. (2) vanish. Within this assumption, where CI is considered to be the unique mechanism creating components $3lnl'$ with $n\geqslant 10$, the influence of the production mechanisms on the average yields $a_{3,\geqslant 10}$ and $\omega_{3,n\geqslant 10}$ can be neglected.

The last terms of the summations in Eqs. (2), i.e., $\sigma_{4,4}(1-\tau)a_{4,4}$ and $\sigma_{4,4}(1-\tau)\omega_{4,4}$, account, respectively, for Auger and radiative emission from the components $4l4l'$. The average fluorescence yield $\omega_{4,4}$ was found to be about 0.1 [25].

To solve the above system of equations [Eqs. (2)], the Auger yields $a_{n,n'}$ are replaced by $(1-\omega_{n,n'})$ in Eq. (2a). Then, since the contribution of AE to the production of states $3lnl'$ with n larger than 10 is presently supposed to be negligible $(\sigma_{3,n\geqslant 10}=0)$, only two unknown parameters remain, i.e., $\sigma_{4,4}$ and $\omega_{3,n\geqslant 10}$. It should be kept in mind that the solutions of the system of equations [Eqs. (2)] represent the maximum values for $\sigma_{4,4}$ and $\omega_{3,n\geqslant 10}$. In the following, the present approximation neglecting the contribution of AE in the creation of the components $3lnl'$ $(n\geqslant 10)$ will be shown to not affect significantly our results. The role of AE in the production of the states $3lnl'$ $(n\geqslant 10)$ is treated in more detail in the Appendix.

C. Contributions to radiative stabilization

The different contributions to radiative stabilization with respect to the total double-capture cross section are based on the experimental cross sections given in Table I. The contribution that follows from the radiative decay of the near-equivalent electron configurations $3lnl'$ $(n=4-5)$ and $4lnl'$ $(n=4-6)$ is denoted by the letter y_E^x. The contribution attributed to the nonequivalent electron configurations $3lnl'$ $(n\geqslant 6)$ is labeled y_N^x. The contribution to stabilization originating from the decay of the configurations $3lnl'$ $(n=6-9)$ created by the dielectronic process AE is referred to as $y_{N(\mathrm{AE})}^x$. Correspondingly, the contribution due to the high-lying Rydberg states $3lnl'$ $(n\geqslant 10)$ produced by CI in the postcollisional and asymptotic regions is denoted $y_{N(\mathrm{CI})}^x$. These different contributions to stabilization can be written as follows [16]:

$$y_E^x=\frac{\Sigma_{n\leqslant 5}\sigma_{3,n}\omega_{3,n}+\sigma_{4,4}(1-\tau)\omega_{4,4}+\Sigma_{n\leqslant 6}\sigma_{4,n}\omega_{4,n}}{\sigma_{\mathrm{tot}}}, \tag{3}$$

$$y_{N(\mathrm{AE})}^x=\frac{\Sigma_{n\geqslant 6}\sigma_{3,n}\omega_{3,n}}{\sigma_{\mathrm{tot}}} \tag{4a}$$

$$y_{N(\mathrm{CI})}^x=\frac{\sigma_{4,4}\tau\omega_{3,n\geqslant 10}}{\sigma_{\mathrm{tot}}} \tag{4b}$$

where σ_{tot} is the total cross section including all double-capture processes, and $\omega_{n,n'}$ is the average fluorescence yield associated with the configurations $nln'l'$ summed over l and l' (Table I). Equation (3) refers to the near-equivalent electron configurations, while Eqs. (4) correspond to the configurations of nonequivalent electrons.

It should be recalled that the results for $\sigma_{4,4}$ and $\omega_{3,n\geqslant 10}$ are maximum values evaluated by neglecting the cross section $\sigma_{3,n\geqslant 10}$ for producing Rydberg states $3lnl'$ (with $n\geqslant 10$) by means of the AE process (see Sec. II B 2). Therefore, the present analysis provides an upper limit for the CI contribution $y_{N(\mathrm{CI})}^x$ [Eq. (4b)] and, hence, a minimum value for the collisional AE contribution $y_{N(\mathrm{AE})}^x$. However, it is shown in the following that our conclusions are unaffected when the limit values of $y_{N(\mathrm{AE})}^x$ and $y_{N(\mathrm{CI})}^x$ are replaced by actual values.

Lastly, the value for the radiative stabilization with respect to the total double capture is given by the sum of the individual contributions as

$$S=y_E^x+y_{N(\mathrm{AE})}^x+y_{N(\mathrm{CI})}^x. \tag{5}$$

III. RESULTS AND DISCUSSION

The cross sections in Table I show that significant changes occur in the population of the configurations $3lnl'$ and $4lnl'$ $(n\geqslant 4)$ when the projectile energy varies from 1 to 150 keV. At the highest energy studied here, double electron capture creates predominantly states due to near-equivalent electron configurations. The cross sections associated with these states are found to be rather constant for the three collision energies [18]. In contrast, the cross sections for producing the nonequivalent electron configurations $3lnl'$ $(n=6-9)$ increase noticeably with decreasing energy and they become dominant at 10 keV (Table I). At this energy, double electron capture into $3lnl'$ $(n=6-9)$ is found to be significantly larger than that into the overlapping states $4l4l'$ and $3lnl'$ $(n\geqslant 10)$. Moreover, the nonequivalent electron configurations $3lnl'$ continue to be enhanced when the impact energy is further reduced by one order of magnitude down to 1 keV. This finding provides evidence for the fact that the collisional AE process plays a decisive role in double electron capture.

The results obtained for the different contributions to radiative stabilization are given in Table II and shown in Fig. 3. The total radiative stabilization values S for doubly excited states of Ne^{8+} produced in collisions with He are found to range within 0.3–0.4. These stabilization values S agree well with the experimental results obtained using x-ray spec-

TABLE II. Contributions to radiative stabilization originating from the decay of doubly excited states $Ne^{8+}(nln'l')$ $(n=3-4)$ produced in 1- to 150-keV $Ne^{10+}+He$ collisions. The contribution due to the decay of (near-) equivalent electron configurations $nln'l'$ $(n'-n\geq 2)$ is compared to those associated with the nonequivalent electron configurations. The contribution originating from the radiative decay of the configurations $3lnl'$ $(n\geq 6)$ produced by the dielectronic process of autoexcitation is labeled AE. The contribution resulting from the production of components $3lnl'$ $(n\geq 10)$ by means of postcollisional and asymptotic configuration-interaction phenomena is labeled CI. In the last row, the fraction S of ions Ne^{8+} that stabilize radiatively with respect to the total number of doubly excited ions Ne^{8+} is given.

Type of configuration	Mechanism	Configurations $nln'l'$	Contributions to stabilization y^x 1 keV	10 keV	150 keV
(Near-) equivalent		$3lnl'$ and $4lnl'$ $(n\approx 4-5)$	0.05 ± 0.02	0.05 ± 0.02	0.08 ± 0.03
Nonequivalent	AE	$3lnl'$ $(n\geq 6)$	0.24 ± 0.05	0.21 ± 0.04	0.10 ± 0.02
Nonequivalent	CI	$4l4l'\rightarrow 3lnl'$ $(n\geq 10)$	0.08 ± 0.03	0.11 ± 0.04	0.14 ± 0.05
Total stabilization S			0.4 ± 0.1	0.4 ± 0.1	0.3 ± 0.1

troscopy [10] as well as recoil-ion-momentum spectroscopy [17,19].

Considering the individual contributions to radiative stabilization, it is seen in Fig. 3 that y_E^x attributed to the near-equivalent electron configurations is rather constant with respect to the variation of the collision energy. The radiative decay of these configurations gives rise to the smallest contribution to stabilization in comparison with the contributions $y_{N(\mathrm{AE})}^x$ and $y_{N(\mathrm{CI})}^x$. Previously [16], the relative cross sections as well as the fluorescence yields associated with the near-equivalent electron states were overestimated by a factor of about 1.5, and this led to an overestimation of the contribution y_E^x. Also, as noted in Sec. II B 1, the average fluorescence yields associated with the near-equivalent electron states are expected to be sensitive to a small energy dependence of the corresponding Auger yields. Hence, in addition to the error bars reported in Fig. 3, further uncertainties occur for y_E^x. Thus, within the experimental uncertainties, we conclude that in the present energy range the contribution y_E^x is practically equal to the CI contribution $y_{N(\mathrm{CI})}^x$ (Fig. 3).

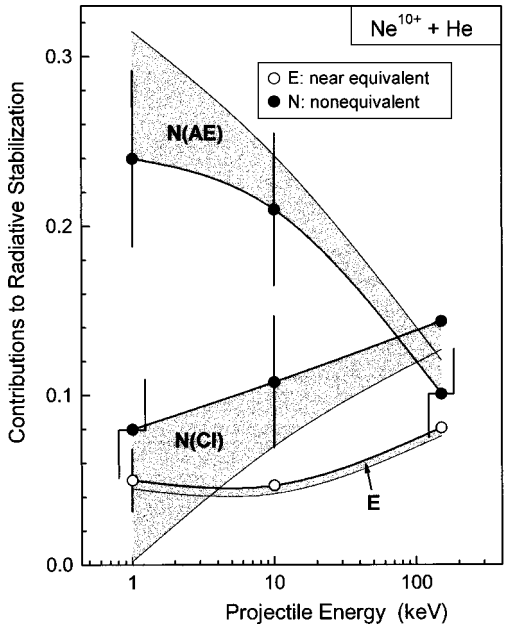

FIG. 3. Contributions to stabilization originating from radiative decay of doubly excited states $Ne^{8+}(nln'l')$ $(n=3-4)$ produced in 1- to 150-keV $Ne^{10+}+He$ collisions. The contribution due to the decay of near-equivalent electron configurations $(n'-n\geq 2)$ is compared to those associated with the nonequivalent electron configurations. The contribution originating from the configurations $3lnl'$ $(n\geq 6)$ produced by the dielectronic process of autoexcitation is labelled AE. The contribution resulting from the production of components $3lnl'$ $(n\geq 10)$ by means of postcollisional and asymptotic configuration-interaction phenomena is labeled CI. The error bars refer to the relative experimental uncertainties, while the shaded regions illustrate the model uncertainties [Eqs. (2)] caused by neglecting the contribution of AE in the production of $3lnl'$ $(n\geq 10)$. These shaded regions indicate the ranges in which the actual values for $y_{E,N}^x$ are expected when the estimated AE contribution for creating $3lnl'$ $(n\geq 10)$ is included (see Appendix). The curves are to guide the eye.

In contrast to the near-equivalent electron configurations, for the configurations $3lnl'$ $(n=6-9)$ significant variations occur with varying collision energy (Fig. 3). At the highest energy of 150 keV, the contribution $y_{N(\mathrm{AE})}^x$ is found to be roughly equal to y_E^x and $y_{N(\mathrm{CI})}^x$. However, with decreasing projectile energy the AE contribution $y_{N(\mathrm{AE})}^x$ increases strongly and it becomes the major contribution at 10 keV. This increase of $y_{N(\mathrm{AE})}^x$ originating from an enhanced production of configurations $3lnl'$ $(n=6-9)$ continues when the impact energy further decreases down to 1 keV. At this energy, the contribution $y_{N(\mathrm{AE})}^x$ for the AE process is found to be 2.5 times larger than $y_{N(\mathrm{CI})}^x$ corresponding to the CI phenomena.

In the present analysis, the average fluorescence yields attributed to the nonequivalent electron configurations $3lnl'$ $(n=6-9)$ have been assumed to be independent of the collision energy (see Sec. II B 1). We expect that the uncertainties caused by this latter assumption do not exceed those for the experimental cross sections and, thus, do not to affect significantly the results for $y_{N(\mathrm{AE})}^x$. In addition, it is recalled that in this study the production of Rydberg states $3lnl'$ with $n\geq 10$ by means of the AE process has been assumed to be negligible. However, as indicated by the shaded regions in Fig. 3, when AE contributions to the production of the states $3lnl'$ $(n\geq 10)$ are taken into account

(see Appendix), the value for $y^x_{N(\mathrm{AE})}$ is increased, whereas $y^x_{N(\mathrm{CI})}$ is decreased. Therefore, the present conclusion about the dominance of the $y^x_{N(\mathrm{AE})}$ contribution is unaffected by the present simplifying assumptions. At 150 keV the relative importance of $y^x_{N(\mathrm{AE})}$ and $y^x_{N(\mathrm{CI})}$ are about equal within the uncertainties of the data. However, the present results obtained at impact energies of a few keV give clear evidence for the predominance of radiative emission from the states $3lnl'$ $(n=6-9)$ produced by the collisional AE process. The enhancement as well as the dominance of $y^x_{N(\mathrm{AE})}$ found at very low energies confirm the major conclusions we made initially for 10 keV projectiles [16].

The CI phenomena may enhance the $4l4l'$ contribution to stabilization by creating components $3lnl'$ $(n\geqslant 10)$ with large fluorescence yields. Hence, based on the assumption that the production of $4l4l'$ is predominant in 10-keV $Ne^{10+}+He$ collisions, it has previously been claimed that the major contribution to stabilization originates from the Rydberg components $3lnl'$ $(n\geqslant 10)$ [21]. This statement is found to be incorrect in view of the present spectra and analysis. For impact energies of 1 and 10 keV, the contribution $y^x_{N(\mathrm{CI})}$ is only about one-quarter of the total amount S of the radiative stabilization (Table II). At energies of 1 and 10 keV, the states $3lnl'$ $(n=6-9)$ produced by the dielectronic process AE dominate the radiative stabilization process.

IV. CONCLUSION

In the present paper, the mechanisms responsible for the production of radiative stabilization in $Ne^{10+}+He$ collisions are studied. The main objective of this work is to evaluate radiative stabilization at collision energies which are one order of magnitude lower than those previously investigated in Ref. [16]. Thus, projectiles with an energy of 1 keV were investigated to compare with the higher energies of 10 and 150 keV studied earlier. The results for these latter energies are revised by replacing theoretical Auger and fluorescence yields [20] with recent experimental data [19,28]. Thus, the different contributions to radiative stabilization are extracted here by combining the experimental Auger and fluorescence yields [19,28] with Auger emission cross sections [18] recently measured by using the method of electron spectroscopy. Effort is devoted to treat the collisional effects in the electron transfer mechanisms together with the postcollisional and asymptotic phenomena of configuration interaction.

The total amount of radiative stabilization varies only slightly with collision energy. However, it is shown that for impact energies of a few keV double-electron capture into the states with the configurations $3lnl'$ $(n=6-9)$ gives the major contribution to radiative stabilization. In particular, the contribution due to the dielectronic process AE increases strongly when the projectile energy decreases from 150 to 1 keV. At the lowest energy of 1 keV, the contribution to radiative stabilization due to the collisional AE process is about 2.5 times larger than those attributed to post-collisional and asymptotic CI phenomena (Fig. 3). Hence, our major conclusion made previously for 10 keV projectiles on the dominance of the AE contribution [16] is confirmed here for the energy of 1 keV.

On the basis of theoretical results [20], the *average* fluorescence yields $\omega_{n,n'}$ attributed to the configurations $nln'l'$ (summed over the angular momenta l and l') are assumed to be independent of the collision energy. However, the l and l' populations may depend on the impact energy, leading to a variation of the fluorescence yields $\omega_{n,n'}$ with respect to the collision energy. Although an energy dependence of the yields $\omega_{n,n'}$ are not expected to affect the present conclusion on the dominance of the AE contribution, it would be helpful to investigate this possible energy dependence so as to improve the analysis of the different contributions to radiative stabilization.

ACKNOWLEDGMENTS

It is a pleasure to thank J. A. Tanis for fruitful comments on the manuscript. We would like to thank also M. Abdallah, C. L. Cocke, L. Adoui, A. Cassimi, X. Fléchard, and D. Hennecart for communicating results prior to publication. This work was performed within the framework of the European Collaboration Research Program PROCOPE under Contract No. 95060. One of us (J.-Y.C.) acknowledges the support of the Alexander-von-Humboldt Foundation, Germany. We are also indebted to the Hungarian-German Intergovernmental Collaboration in Science and Technology (Project No. B/129) for their support.

APPENDIX: MECHANISMS FOR THE CREATION OF THE STATES $3lnl'$ WITH $n\geqslant 10$

In this appendix, the attempt is made to analyze the relative importance of AE and CI in the production of the high-lying Rydberg states $3lnl'$ $(n\geqslant 10)$. It is recalled that these Rydberg states $3lnl'$ $(n\geqslant 10)$ overlap in energy with the states $4l4l'$ (Fig. 2). The average fluorescence yield ω_{os} attributed to these overlapping states depends on the relative population of the components $4l4l'$ and $3lnl'$ $(n\geqslant 10)$. In other words, since the CI phenomena require an initial population of $4l4l'$, the fluorescence yield ω_{os} depends on the relative importance of CI compared with that of AE.

To study the relative contributions of CI and AE in the production of the Rydberg states $3lnl'$ $(n\geqslant 10)$, it is helpful to evaluate the average fluorescence yield ω_{os} under two extreme hypotheses, where either the CI or the AE contribution to the creation of the states $3lnl'$ $(n\geqslant 10)$ is assumed to be negligible. First, if the cross section $\sigma_{4,4}$ for producing $4l4l'$ is equal to zero, postcollisional and asymptotic CI phenomena cannot contribute to the production of Rydberg components $3lnl'$ $(n\geqslant 10)$ [31]. In this particular case, since the weight of $\omega_{4,4}$ vanishes, the yield ω_{os} reaches the value of $\omega_{3,n\geqslant 10}$. This situation, where AE is the unique process leading to the states $3lnl'$ $(n\geqslant 10)$, is depicted by curve *a* in Fig. 4. On the other hand, if the role of AE in the creation of $3lnl'$ $(n\geqslant 10)$ is negligible (i.e., $\sigma_{3,n\geqslant 10}\rightarrow 0$), for a given value of $\omega_{3,n\geqslant 10}$ the yield ω_{os} becomes equal to $\tau\omega_{3,n\geqslant 10}+(1-\tau)\omega_{4,4}$ [Eq. (4b)]. This second value of ω_{os} is given by curve *b* in Fig. 4. Hence, the vicinity of curve *b* in Fig. 4 corresponds to the predominance of the CI phenomena. Note that this latter value of ω_{os} is larger than $\omega_{4,4}$ because the fraction τ of the initial $4l4l'$ population that goes into com-

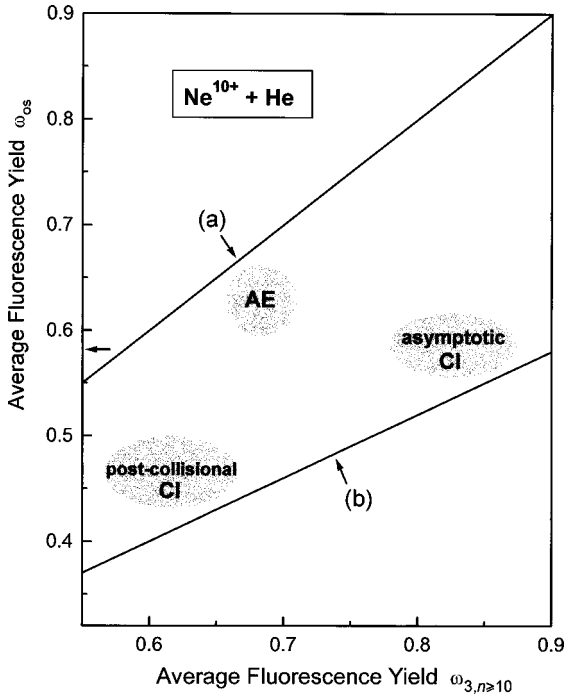

FIG. 4. Upper and lower limits of the average fluorescence yield ω_{os} associated with the region of overlapping states. The upper limit of ω_{os} (curve *a*) results from the hypothesis that the collisional AE process is the unique mechanism for producing the Rydberg components $3lnl'$ $(n \geqslant 10)$. On the other hand, the hypothesis that the Rydberg components are due to CI phenomena leads to the lower limit of ω_{os} (curve *b*.) Since the postcollisional CI produces $3lnl'$ states with smaller *n* values than asymptotic CI, postcollisional CI is likely to lead to lower values for $\omega_{3,n\geqslant 10}$ than the asymptotic phenomenon (the smaller the *n* value, the smaller the corresponding average fluorescence yield [25]). These extrema for ω_{os} are independent of the projectile energy (see text).

ponents $3lnl'$ $(n \geqslant 10)$ by CI phenomena differs from zero [23].

As the postcollisional CI produces $3lnl'$ states with smaller *n* values than the asymptotic CI [25], the postcollisional CI is likely to lead to lower values for $\omega_{3,n\geqslant 10}$ than the asymptotic phenomenon (Fig. 4). Thus, to investigate further the mechanisms responsible for producing the components $3lnl'$ $(n \geqslant 10)$, it is useful to evaluate the average yield $\omega_{3,n\geqslant 10}$. By neglecting the AE cross section $\sigma_{3,n\geqslant 10}$, the foregoing analysis (Sec. II B 2) provides maximum values for the yield $\omega_{3,n\geqslant 10}$ (as well as for the cross section $\sigma_{4,4}$). Nevertheless, the AE cross section $\sigma_{3,n\geqslant 10}$ can be estimated by means of an extrapolation by fitting the function $n^{-\alpha}$ to the intensities of the states $3lnl'$ with $n=6-9$. Then, approximate values for the average fluorescence yield $\omega_{3,n\geqslant 10}$ (and also for $\sigma_{4,4}$) can be extracted from Eqs. (2) in Sec. II B 2. Such estimated values for $\sigma_{3,n\geqslant 10}$, $\omega_{3,n\geqslant 10}$, and $\sigma_{4,4}$ have been included in Eqs. (3) and (4) of Sec. III C to evaluate the model uncertainties in the foregoing analysis (see Fig. 3).

For the energy of 150 keV, the average fluorescence yield ω_{os} has recently been measured by Abdallah and co-workers [19,28] to be $\omega_{os}=0.58$. From the ω diagram in Fig. 4, this number implies that the average fluorescence yield $\omega_{3,n\geqslant 10}$ ranges from 0.6 to 0.8 when both AE and CI are assumed to contribute significantly to the production of the Rydberg components $3lnl'$ $(n \geqslant 10)$. Moreover, after evaluation of the AE cross section $\sigma_{3,n\geqslant 10}$ by extrapolating the function $n^{-\alpha}$, the fluorescence yield $\omega_{3,n\geqslant 10}$ has been found to be about 0.7–0.8. Then, for $\omega_{3,n\geqslant 10}\sim 0.75$ and $\omega_{os}=0.58$, the diagram suggests that the role of the asymptotic CI phenomenon in the production of $3lnl'$ $(n \geqslant 10)$ dominates that of the postcollisional CI phenomenon. Thus, in accordance with the results of Van der Hart *et al.* [25], the contribution $y^{x}_{N(\mathrm{CI})}$ obtained at 150 keV is likely to be due to the radiative decay of Rydberg states whose production occurs mainly in the asymptotic region.

Next, when the projectile energy decreases, the collisional AE process is likely to gain importance in the production of $3lnl'$ states with $n \geqslant 10$, as for the case of the states $3lnl'$ $(n=6-9)$ (Table I). In the spectra of Fig. 2, the observation of a high-intensity peak at the electron energy corresponding to $3l10l'$ supports this expectation. From the ω diagram in Fig. 4, an enhancement of the AE contribution in the production of the Rydberg states $3lnl'$ $(n \geqslant 10)$ may result in an increase of the fluorescence yield ω_{os} [32]. Thus, further experiments to measure the projectile-energy dependence of the fluorescence yield ω_{os}, especially for impact energies of a few keV, may provide additional information about the role of AE for the particular case of the Rydberg states $3lnl'$ $(n \geqslant 10)$.

[1] A. Bordenave-Montesquieu, P. Benoit-Cattin, A. Gleizes, A. I. Marrakchi, S. Dousson, and D. Hitz, J. Phys. B **17**, L127 (1984); L223 (1984).

[2] N. Stolterfoht, C. C. Havener, R. A. Phaneuf, J. K. Swenson, S. M. Shafroth, and F. W. Meyer, Phys. Rev. Lett. **57**, 74 (1986).

[3] S. Bliman, J. J. Bonnet, D. Hitz, T. Ludcec, M. Druetta, and M. Mayo, Nucl. Instrum. Methods Phys. Res. B **27**, 579 (1987).

[4] P. Boduch, M. Chantepie, D. Hennecart, X. Husson, H. Kucal, D. Lecler, and I. Lesteven-Vaisse, J. Phys. B **22**, L377 (1989).

[5] D. Vernhet, A. Chetioui, J. P. Rozet, C. Stephan, K. Wohrer, A. Touati, M. F. Politis, P. Bouisset, D. Hitz, and S. Dousson, J. Phys. B **22**, 1603 (1989).

[6] N. Stolterfoht, K. Sommer, J. K. Swenson, C. C. Havener, and F. W. Meyer, Phys. Rev. A **42**, 5396 (1990).

[7] P. Roncin, M. N. Gaboriaud, and M. Barat, Europhys. Lett. **16**, 551 (1991).

[8] R. Hoekstra, J. P. M. Beijers, F. J. de Heer, and R. Morgenstern, Z. Phys. D **25**, 209 (1993).

[9] F. Fremont, H. Merabet, J.-Y. Chesnel, X. Husson, A. Lepoutre, D. Lecler, G. Rieger, and N. Stolterfoht, Phys. Rev. A **50**, 3117 (1994).

[10] S. Martin, J. Bernard, Li Chen, A. Denis, and J. Désesquelles, Phys. Rev. A **52**, 1218 (1995).

[11] H. Bachau, P. Roncin, and C. Harel, J. Phys. B **25**, L109 (1992).
[12] H. W. van der Hart and J. E. Hansen, J. Phys. B **27**, L395 (1994); H. W. van der Hart, N. Vaeck, and J. E. Hansen, *ibid.* **27**, 3489 (1994).
[13] N. Stolterfoht, Phys. Scr. **T51**, 39 (1994).
[14] H. Merabet, F. Fremont, J.-Y. Chesnel, G. Cremer, X. Husson, D. Lecler, A. Lepoutre, G. Rieger, and N. Stolterfoht, Nucl. Instrum. Methods Phys. Res. B **99**, 75 (1995).
[15] J. P. Desclaux, Nucl. Instrum. Methods Phys. Res. B **98**, 18 (1995).
[16] J.-Y. Chesnel, H. Merabet, F. Frémont, G. Cremer, X. Husson, D. Lecler, G. Rieger, A. Spieler, M. Grether, and N. Stolterfoht, Phys. Rev. A **53**, 4198 (1996).
[17] X. Fléchard, S. Duponchel, L. Adoui, A. Cassimi, P. Roncin, and D. Hennecart, J. Phys. B **30**, 3697 (1997).
[18] J.-Y. Chesnel, B. Sulik, H. Merabet, C. Bedouet, F. Frémont, X. Husson, M. Grether, A. Spieler, and N. Stolterfoht, Phys. Rev. A **57**, 3546 (1998).
[19] M. Abdallah, C.L. Cocke, S. Kravis, E. C. Montenegro, R. Moshammer, L. Saleh, J. Ullrich, S. L. Varghese, W. Wolff, and H. Wolf, in Proceedings of the XIV International Conference on the Application of Accelerators in Research and Industry, Denton, Texas, 1996, edited by J. L. Duggan and I. L. Morgan, AIP Conf. Proc. No. **392** (AIP, New York, 1997), p. 209.
[20] H. Merabet, G. Cremer, F. Fremont, J.-Y. Chesnel, and N. Stolterfoht, Phys. Rev. A **54**, 372 (1996).
[21] P. Roncin, M. N. Gaboriaud, Z. Szilagyi, and M. Barat, in Proceedings of the XVIII International Conference on the Physics of Electronic and Atomic Collisions, Aarhus, Denmark, 1993, edited by T. Andersen, B. Fastrup, F. Folkmann, J. Knudsen, and N. Andersen, AIP Conf. Proc. No. **295** (AIP, New York, 1993), p. 537.
[22] A. K. Kazansky, J. Phys. B **25**, L381 (1982); A. K. Kazansky and P. Roncin, *ibid.* **27**, 5537 (1994).
[23] I. Sánchez and H. Bachau, J. Phys. B **28**, 795 (1995).
[24] N. Vaeck and J. E. Hansen, J. Phys. B **26**, 2977 (1993); N. Vaeck, H. W. van der Hart, and J. E. Hansen, in Proceedings of the XVIII International Conference on the Physics of Electronic and Atomic Collisions, Aarhus, Denmark, 1993, edited by T. Andersen, B. Fastrup, F. Folkmann, J. Knudsen, and N. Andersen, AIP Conf. Proc. No. **295** (AIP, New York, 1993), p. 794.
[25] H. W. van der Hart, J. E. Hansen, H. Bachau, and I. Sànchez, J. Phys. B **30**, 203 (1997).
[26] N. Stolterfoht, Z. Phys. **248**, 81 (1971); **248**, 92 (1971).
[27] A. Itoh, T. Schneider, G. Schiwietz, Z. Roller, H. Platten, G. Nolte, D. Schneider, and N. Stolterfoht, J. Phys. B **16**, 3965 (1983).
[28] M. Abdallah and C. L. Cocke (private communication).
[29] H. Merabet, Ph.D. thesis, University of Caen, France, 1996.
[30] D. Hennecart, X. Fléchard, F. Frémont, A. Lepoutre, S. Duponchel, L. Adoui, and A. Cassimi, *Photonic, Electronic and Atomic Collisions; Invited Papers of the Twentieth International Conference on the Physics of Electronic and Atomic Collisions, Vienna, Austria, 1997*, edited by F. Aumayr and H. P. Winter (World Scientific, Singapore, 1998), p. 557, and private communication.
[31] Another possibility to assume that CI plays a negligible role is to consider that the fraction τ of the initial population $4l4l'$ which goes into the Rydberg states $3lnl'$ ($n \geqslant 10$) is equal to zero. However, this eventuality is not considered here, since a value of 0.6 has been recently found for the fraction τ [23].
[32] An enhancement of AE may also result in a decrease of the average fluorescence yield $\omega_{3,n \geqslant 10}$, by favoring lower n values and, thus, smaller fluorescence yields $\omega_{3,n}$.